ENVIRONMENTAL RESEARCH
LETTERS

Tropical cloud-radiative changes contribute to robust climate change-induced jet exit strengthening over Europe during boreal winter

To cite this article before publication: Nicole Albern *et al* 2021 *Environ. Res. Lett.* in press https://doi.org/10.1088/1748-9326/ac13f0

Tropical cloud-radiative changes contribute to robust climate change-induced jet exit strengthening over Europe during boreal winter

Nicole Albern[1], Aiko Voigt[2,3], Joaquim G. Pinto[1]

[1] Institute of Meteorology and Climate Research - Department Troposphere Research, Karlsruhe Institute of Technology, Karlsruhe, Germany

[2] Department of Meteorology and Geophysics, University of Vienna, Vienna, Austria

[3] Lamont-Doherty Earth Observatory, Columbia University, New York, New York, USA

Keywords: cloud-circulation coupling, regional climate change, North Atlantic jet stream, model hierarchy, boreal winter

Abstract

The North Atlantic jet stream is projected to extend eastward towards Europe in boreal winter in response to climate change. We show that this response is robust across a hierarchy of climate models and climate change scenarios. We further show that cloud-radiative changes contribute robustly to the eastward extension of the jet stream in three atmosphere models, but lead to model uncertainties in the jet stream response over the North Atlantic. The magnitude of the cloud contribution depends on the model, consistent with differences in the magnitude of changes in upper-tropospheric cloud-radiative heating. We further study the role of regional cloud changes in one of the three atmosphere models, i.e. the ICON model. Tropical cloud-radiative changes dominate the cloud impact on the eastward extension of the jet stream in ICON. Cloud-radiative changes over the Indian Ocean, western tropical Pacific, and eastern tropical Pacific contribute to this response, while tropical Atlantic cloud changes have a minor impact. Our results highlight the importance of upper-tropospheric tropical clouds for the regional circulation response to climate change over the North Atlantic-European region and uncertainty therein.

1 Introduction

The North Atlantic eddy-driven jet stream is expected to undergo substantial changes in response to climate change. Climate models project that the annual-mean jet stream will shift poleward (e.g., Chang et al., 2012; Barnes and Polvani, 2013; Vallis et al., 2015), and reanalyses indicate that the vertical wind shear will increase due to changes in meridional temperature gradients (Lee et al., 2019). However, the jet response varies strongly between seasons. While a poleward jet shift is found during most seasons, the jet is projected to extend eastward towards Europe rather than to shift poleward during boreal winter (December to February, DJF) (e.g., Pinto et al., 2007; Woollings and Blackburn, 2012; Zappa et al., 2013; Simpson et al., 2014; Harvey et al., 2015; Zappa et al., 2015). As shown in Harvey et al. (2020), this wintertime response is found in the model-mean of coupled climate models that contributed to phases 3, 5, and 6 of the Coupled Model Intercomparison Project (CMIP; Meehl et al., 2000; Taylor et al., 2012; Eyring et al., 2016). The eastward extension is robust across coupled climate models (Simpson et al., 2014) but its magnitude remains uncertain (Shepherd, 2014). Over the North Atlantic, the response is uncertain as some models exhibit a poleward jet shift while others exhibit an equatorward jet shift (Barnes and Polvani, 2013; Shepherd, 2014).

The eastward extension of the North Atlantic jet stream in response to climate change co-occurs with an eastward extension of the North Atlantic storm track (Harvey et al., 2020). The responses of the jet stream and storm track are of large social and economic interest, with both positive and negative consequences for Europe. On the one hand, the increases in wind speed will result in a higher wind energy production over Northern Europe (Hueging et al., 2013; Reyers et al., 2016; Carvalho et al., 2017; Moemken et al., 2018). On the other hand, an increase in winter storms over Europe will increase the potential for severe losses due to storminess, flooding after extreme precipitation events, and other damages (Leckebusch et al., 2007; Pinto et al., 2012; Catto et al., 2019).

Changes in cloud-radiative properties affect the zonal wind response to climate change as clouds and the atmospheric circulation are strongly coupled via radiation (cf. review by Voigt et al., 2021, and references therein). This cloud-radiative impact acts via changes in the surface energy balance and changes in the atmospheric energy balance, referred to as surface pathway and atmospheric pathway of the cloud-radiative impact, respectively (Voigt et al., 2019). Here, we focus on the atmospheric pathway of the cloud-radiative impact. The atmospheric pathway can be quantified by using the cloud-locking method together with prescribed sea-surface temperatures (SSTs). Prescribing SSTs disables the surface pathway, as then cloud-induced changes in the surface energy balance over the ocean no longer affect SSTs. As a result, the circulation response can be decomposed into contributions from changes in cloud-radiative properties and SSTs (e.g., Voigt and Shaw, 2015, 2016; Voigt and Albern, 2019).

The atmospheric pathway of the cloud-radiative impact contributes substantially to the zonal wind and jet stream responses in atmosphere models in the zonal-mean perspective (Voigt et al., 2019) and across seasons and regions (Albern et al., 2019, 2020). In particular, Albern et al. (2019) showed for the ICON model that about one quarter of the DJF zonal wind response at 850 hPa across the midlatitudes can be attributed to changes in cloud-radiative properties. Further, Albern et al. (2020) showed that tropical cloud-radiative changes dominate the cloud impact on the zonal wind response in the same model. Yet, while the zonal-mean response was studied in several models, the impact of cloud-radiative changes on the regional zonal wind and jet responses has so far only been quantified in the ICON model.

Here, we study the role of cloud-radiative changes on the eastward extension of the North Atlantic jet stream towards Europe under climate change. We first investigate a hierarchy of climate models and simulation setups to identify which aspects of the climate change response are robust. We then study the impact of cloud-radiative changes on the zonal wind response in three atmosphere models, and identify how much of the robust response can be attributed to cloud-radiative changes in each model. Finally, we focus on the ICON model to assess which regional cloud-radiative changes are most important for the zonal wind response over Europe.

2 Data and Methods

2.1 CMIP5 Simulations

We investigate the zonal wind response to climate change across models and climate change scenarios of varying complexity. The most complex models in our model hierarchy are coupled climate models. We study the historical (years 1975-2004) and RCP8.5 simulations (years 2070-2099) from 37 coupled climate models that participated in CMIP5 (Taylor et al., 2012). Reducing the models' complexity, we further investigate output from eleven atmosphere-only climate models with prescribed SSTs and sea ice cover that performed the Amip, Amip4K and AmipFuture simulations (years 1979-2008) of CMIP5 (Taylor et al., 2012). In these simulations, climate change is mimicked by increasing SSTs. The Amip4K climate change scenario is the most idealized scenario in our hierarchy as it simulates climate change by a uniform 4 K SST increase. The AmipFuture simulations, in contrast, use an SST pattern derived from coupled climate models (Taylor et al., 2009, 2012). The investigated CMIP5 models are listed in Tab. S1.

2.2 Cloud-locking Simulations

We investigate simulations with the atmospheric components of the ICON model (Zängl et al., 2015), and the low resolution versions of the MPI-ESM (Giorgetta et al., 2013; Stevens et al., 2013) and IPSL-CM5A (Dufresne et al., 2013) models that applied the cloud-locking (ICON) or cloud- and water vapor-locking (MPI-ESM and IPSL-CM5A) methods to determine how much of the zonal wind response can be attributed to changes in cloud-radiative properties. The ICON simulations with locked clouds and interactive water vapor are taken from Albern et al. (2019). The MPI-ESM and IPSL-CM5A simulations with locked clouds and locked water vapor are taken from Voigt et al. (2019). The simulations were performed analogously to the Amip simulations, but use climatological SSTs and sea ice cover. They have a length of 27 years (IPSL-CM5A), 28 years (MPI-ESM), and 30 years (ICON), respectively. For each simulation, the first year is excluded from the analysis to avoid effects from model initialization. In accordance with the Amip4K simulations, climate change was mimicked by a uniform 4 K SST increase (cf. Albern et al. (2019) and Voigt et al. (2019) for details of the simulations' setups). Detailed descriptions of the locking method are given, for example, in Voigt and Shaw (2015) and Albern et al. (2019).

For the cloud-locking method, first the radiative properties of clouds have to be stored for the present-day and climate-change simulations. Second, four simulations have to be performed, in which SST (T) and cloud-radiative properties (C) are prescribed to either of the two climate states. The total locked response of any given variable X is then

$$\Delta X_{\text{total, free vapor}} = X_{\text{T2C2}} - X_{\text{T1C1}}, \tag{1}$$

where the indices indicate whether T and C are taken from the present-day (1) or climate-change (2) simulation. The cloud-radiative impact via the atmospheric pathway is calculated as (Albern et al., 2019)

$$\Delta X_{\text{cloud, free vapor}} = \frac{1}{2}\left[(X_{\text{T1C2}} - X_{\text{T1C1}}) + (X_{\text{T2C2}} - X_{\text{T2C1}})\right]. \tag{2}$$

Analogously, the radiative properties of clouds and water vapor have to be stored for the cloud- and water vapor-locking method, and eight simulations have to be performed, in which T, C, and water vapor-radiative properties (W) are prescribed to either of the two climate states. The total locked response for simulations with prescribed clouds and water vapor is

$$\Delta X_{\text{total, locked vapor}} = X_{\text{T2C2W2}} - X_{\text{T1C1W1}}, \tag{3}$$

and the cloud-radiative impact via the atmospheric pathway is calculated as (Voigt and Shaw, 2015)

$$\begin{aligned}\Delta X_{\text{cloud, locked vapor}} = \frac{1}{4}[&(X_{\text{T1C2W1}} - X_{\text{T1C1W1}}) + (X_{\text{T1C2W2}} - X_{\text{T1C1W2}}) \\ &+(X_{\text{T2C2W1}} - X_{\text{T2C1W1}}) + (X_{\text{T2C2W2}} - X_{\text{T2C1W2}})].\end{aligned} \tag{4}$$

Note that for all investigated models the residuals between the total response with interactive clouds/water vapor and the total response with locked clouds/water vapor, which arise due to the decoupling of clouds/water vapor and the circulation when applying the locking methods, were found to be small (Albern et al., 2019; Voigt and Albern, 2019; Voigt et al., 2019).

It is meaningful to directly compare the cloud-radiative impact from ICON simulations with interactive water vapor to that from MPI-ESM and IPSL-CM5A simulations with locked water vapor because the cloud-radiative impact is largely insensitive to the treatment of water vapor (Voigt and Albern, 2019). Investigating the annual-mean zonal-mean atmospheric circulation, Voigt and Albern (2019) showed for ICON that the estimated cloud-radiative impact on the responses of various circulation metrics, including the position and strength of the jet stream, hardly depends on whether water vapor is interactive or prescribed. Investigating the regional zonal wind response at 850 hPa, Δu_{850}, we find that the treatment of water vapor in the ICON simulations of Voigt and Albern (2019) has a negligible effect on the pattern and magnitude of the total zonal wind response and the cloud-radiative impact on Δu_{850} over the North Atlantic-European region during winter (Fig. S1).

For the ICON model, we do not only determine the impact of global cloud changes but also the impact of regional cloud changes. In addition to the four above mentioned simulations for the global cloud impact, four more simulations are performed for each region of interest (Albern et al., 2020). In these simulations, clouds in the region of interest (marked by subscript a in Eq. 5) and clouds in the rest of the world (marked by subscript b) are prescribed to values from either the control simulation or the climate-change simulation. A more detailed discussion of the methodology can be found in Albern et al. (2020).

Based on these simulations, the impact of regional cloud changes is calculated as

$$\begin{aligned}\Delta X_{\text{clouds, reg}} = \frac{1}{4}[&(X_{\mathrm{T1C}_a\mathrm{2C}_b\mathrm{1}} - X_{\mathrm{T1C}_a\mathrm{1C}_b\mathrm{1}}) + (X_{\mathrm{T1C}_a\mathrm{2C}_b\mathrm{2}} - X_{\mathrm{T1C}_a\mathrm{1C}_b\mathrm{2}}) \\ &+(X_{\mathrm{T2C}_a\mathrm{2C}_b\mathrm{1}} - X_{\mathrm{T2C}_a\mathrm{1C}_b\mathrm{1}}) + (X_{\mathrm{T2C}_a\mathrm{2C}_b\mathrm{2}} - X_{\mathrm{T2C}_a\mathrm{1C}_b\mathrm{2}})]. \end{aligned} \tag{5}$$

We investigate the regional cloud impacts for the following regions: tropics (30°S-30°N, all longitudes), midlatitudes (30°N-60°N and 30°S-60°S, all longitudes), polar regions (poleward of 60°N/S, all longitudes), North Atlantic-European region (30°N-60°N, 90°W-30°E), western tropical Pacific (30°S-30°N, 120°E-150°W), eastern tropical Pacific (30°S-30°N, 150°W-70°W), tropical Atlantic (30°S-30°N, 70°W-40°E), and Indian Ocean (30°S-30°N, 40°E-120°E), (cf. Fig. S2 for a schematic of the regions).

2.3 Jet Stream

We derive the eddy-driven jet stream from the maximum in the zonal wind at 850 hPa. Based on the zonal wind interpolated linearly onto a 0.01° latitude grid, we perform a quadratic fit around the maximum and the two neighboring grid points, and define the jet latitude φ_{jet} and jet strength u_{jet} as the position and value of the maximum of the quadratic fit (e.g., Barnes and Polvani, 2013; Albern et al., 2019).

3 Results

3.1 Robust Circulation Response and Contribution of Global Cloud-Radiative Changes

We begin by showing which aspects of the circulation response to climate change over the North Atlantic-European region are robust across coupled and atmosphere-only climate models. The top row of Fig. 1 shows the CMIP5 model-mean zonal wind response at 850 hPa, Δu_{850}. In the model mean, all three scenarios show a poleward shift and strengthening of the jet stream over the North Atlantic, and a zonal wind increase over central and northern Europe (Fig. 1a-c). The latter is associated with an eastward extension of the North Atlantic jet stream towards Europe, and commonly referred to as jet exit strengthening. The responses over Europe are robust across models in all three model setups. Over the North Atlantic, however, the models do not agree on the u_{850} increase on the poleward flank of the jet in the coupled models, and on the u_{850} weakening on the equatorward flank of the jet in the atmosphere-only models.

As the CMIP5 model mean, ICON, MPI-ESM, and IPSL-CM5A show the jet exit strengthening over Europe (Fig. 1d-f). However, the region of the jet exit strengthening is model dependent. While the zonal wind increase in MPI-ESM, IPSL-CM5A, and the CMIP5 simulations is strongest over western to central Europe, the zonal wind increase in ICON is largest over the southern half of northern Europe including the North Sea and Baltic Sea regions. The region of the largest zonal wind increase is linked to the tilt of the North Atlantic jet stream, which is larger in ICON and smaller in the other two models and the CMIP5 model mean (cf. thick black dots in Fig. 1).

ICON, MPI-ESM and IPSL-CM5A reflect the CMIP5 model uncertainties over the North Atlantic. ICON shows a poleward jet shift across the North Atlantic, while MPI-ESM and IPSL-CM5A exhibit a jet strengthening over the eastern part of the North Atlantic, and in IPSL-CM5A the jet shifts equatorward over the eastern North Atlantic close to France and the Iberian Peninsula (Fig. 1d-f). The responses in all three models agree well with the robust zonal wind responses in the Amip4K model mean (hatching in Fig. 1d-f).

Fig. 2 contrasts the jet response over Europe (0°-25°E, panels a-c) with the jet response over the North Atlantic (60°W-0°, panels d-f) across the CMIP5 models and ICON, MPI-ESM, and IPSL-CM5A. In both regions, most models exhibit poleward jet shifts of up to 2.5°. Several models exhibit an equatorward jet shift over the North Atlantic which is less pronounced over Europe. Some models (CMCC-CMS and CSIRO-Mk3-6-0 for RCP8.5; bcc-csm1-1, IPSL-CM5B and MIROC5 for Amip-Future and Amip4K) exhibit very large jet shifts of more than 10°. These large jet shifts are excluded from Fig. 2, and are due to the fact that the models exhibit very weak jet streams over Europe, resulting in a weak and flat u_{850} profile that is very sensitive to small wind changes.

While the magnitudes of the jet shifts are similar in both regions, larger differences between the North Atlantic and Europe are found for the jet strength response. In the atmosphere-only models, the jet strengthening over Europe is in most models two to five times larger than over the North Atlantic. The same general behavior is found for the coupled climate models. Yet, several coupled models exhibit only small responses in the jet strength over Europe, reflecting the larger inter-model variability in the more complex coupled models (although this is also partly due to the larger ensemble). In both regions, the jet shift and jet strengthening in ICON, MPI-ESM and IPSL-CM5A lie well within the jet responses of the atmosphere-only CMIP5 models for the Amip4K scenario (Fig. 2c, f).

We now focus on the jet exit strengthening over Europe. Fig. 3 shows the total u_{850} response (reproduced from Fig. 1) and the cloud impact on the u_{850} response in ICON, MPI-ESM, and IPSL-CM5A. The cloud-radiative impact contributes substantially to the jet exit strengthening in all three models (Fig. 3, right). Over the North Atlantic, however, the cloud impact differs between the three models so that it can be considered as one source of uncertainty in the circulation response in this region. This finding is consistent with the non-robust circulation response over the North Atlantic in the CMIP5 models as well as in ICON, MPI-ESM and IPSL-CM5A (cf. Fig. 1).

Even though cloud changes appear to robustly contribute to the jet exit strengthening, the magnitude of the cloud impact varies strongly between the three models, as does the total response (Fig. 3). Further, the relative contribution of the cloud impact to the total u_{850} response is model dependent. Over the European region, for which the signs of the total responses in ICON, MPI-ESM and IPSL-CM5A agree with the sign of the robust response of the CMIP5 models in the Amip4K scenario (50°N-59°N, 4°W-25°E, cf. hatching in Fig. 1d-f), cloud changes contribute about one quarter to the total u_{850} response in ICON and MPI-ESM. In IPSL-CM5A, however, essentially all of the total response in this region can be attributed to cloud-radiative changes. Note that for large parts of the North Atlantic-European region, the pattern of the u_{850} response to cloud changes largely resembles the pattern of the total response in ICON and MPI-ESM. In IPSL-CM5A, in contrast, the cloud impact and total response exhibit quite different spatial structures with an equatorward jet shift and jet strengthening for the total response and a poleward jet shift and jet strengthening for the cloud impact.

To understand the different magnitudes and relative contributions of the cloud-radiative impacts in the three models, we investigate the changes in cloud-radiative heating derived from Partial-Radiative Perturbation (PRP) calculations (Wetherald and Manabe, 1988; Colman and McAvaney, 1997; Voigt and Shaw, 2016; Voigt et al., 2019). The PRP calculations are based on the locked simulations and quantify the changes in temperature tendencies due to changes in cloud-radiative properties under climate change.

In the zonal mean, the largest changes in atmospheric cloud-radiative heating are found in the tropical and midlatitude upper troposphere (Fig. 4a-c). These changes are strongly linked to changes in cloud cover (Voigt and Shaw, 2016; Voigt et al., 2019; Albern et al., 2020), and differences in cloud-radiative heating changes between the models can be linked to differences in present-day cloud cover and in cloud cover response to climate change (Fig. S3). For a direct comparison of cloud-radiative heating changes and cloud cover response cf. Fig. 5g-i in Voigt et al. (2019).

Previous studies proposed that changes in high-level ice clouds play an important role for the response of the midlatitude circulation to climate change (Voigt and Shaw, 2016; Voigt et al., 2019; Albern et al., 2020). Thus, we focus our analysis on the upper troposphere and investigate regional vertical-mean changes in atmospheric cloud-radiative heating for a 200-hPa-thick layer below the DJF tropopause. The qualitative differences in the magnitude and pattern of the change in atmospheric cloud-radiative heating between the models is independent of whether the vertical mean is calculated over a 200 or 300 hPa thick layer below the tropopause.

In all three models, the changes in upper-tropospheric cloud-radiative heating peak over the western tropical Pacific and Maritime Continent (Fig. 4d-f). In ICON and MPI-ESM, there are secondary peaks over the Indian Ocean, while in IPSL-CM5A a secondary peak is found over the central subtropical Pacific of the Southern Hemisphere. The changes in atmospheric cloud-radiative heating in ICON and MPI-ESM are similar in a sense that they are largest in similar tropical regions, while the changes in the midlatitudes and polar regions are small (Fig. 4d-e). This might explain why the relative contributions of the cloud impacts on the u_{850} response in ICON and MPI-ESM are similar. In IPSL-CM5A, the peak in the vertical-mean tropical upper-tropospheric cloud-radiative heating changes is smaller while the changes in the midlatitudes are larger than in ICON and MPI-ESM (Fig. 4f). The increased cloud-radiative heating around the jet stream might explain the larger cloud impact on the u_{850} response in IPSL-CM5A compared to the other two models.

The results suggest that differences in the pattern and magnitude of the upper-tropospheric cloud-radiative heating changes can lead to differences in the u_{850} response in ICON, MPI-ESM and IPSL-CM5A (cf. Fig. 3). As Albern et al. (2020) showed that tropical cloud-radiative changes dominate the u_{850} response to climate change in ICON, the differences in the u_{850} response might be primarily linked to differences in tropical cloud-radiative heating changes. Therefore, we investigate the impact of tropical cloud-radiative changes in more detail in the next section.

3.2 Regional Cloud-Radiative Impact on the Circulation Response in ICON

In this section, we focus on the ICON model to investigate which regional cloud-radiative changes are most important for the global cloud impact. Albern et al. (2020) showed that tropical cloud-radiative changes dominate the annual-mean, wintertime and summertime global cloud-radiative impact on the midlatitude u_{850} response to climate change in ICON (cf. their Fig. 3). Here, we investigate the wintertime u_{850} response over the North Atlantic-European region in more detail. We find that tropical cloud-radiative changes dominate the global cloud-radiative impact over Europe (Fig. 5a), while midlatitude and polar cloud-radiative changes have smaller contributions (Fig. 5b-c). For the European region, where the jet exit strengthening is largest in ICON (52°N-62°N, 4°W-26°E; cf. boxes in Fig. 5), tropical cloud changes actually lead to a larger zonal wind increase than global cloud changes, while about one fifth and one quarter of the jet exit strengthening can be attributed to midlatitude and polar cloud changes, respectively. Note that the sum of the tropical, midlatitude and polar cloud changes overestimates the global cloud impact in the given region by more than 50% due to non-linearities that arise when the cloud-radiative heating is induced individually (Butler et al., 2010), an effect that might be enhanced by gradients in the cloud-radiative properties at the boundaries of the tropical, midlatitude and polar regions (Albern et al., 2020).

Over the North Atlantic, tropical, midlatitude and polar cloud changes all contribute to the poleward jet shift, and tropical cloud changes lead to a significant strengthening of the North Atlantic jet (cf. our Fig. 5a-c and Figs. 5 and 6 in Albern et al., 2020). In contrast, local cloud-radiative changes over the North Atlantic and Europe lead to a slight, non-significant weakening of the zonal wind and jet stream over the North Atlantic-European region (not shown) (cf. Fig. S2a-d for the regions). Thus, remote cloud-radiative changes, in particular those in the tropics, are much more important for the jet stream response over the North Atlantic-European region than local cloud-radiative changes.

We now investigate which tropical region dominates the tropical cloud-radiative impact. Cloud changes over the western tropical Pacific (WP), the eastern tropical Pacific (EP) and the Indian Ocean (IO) (cf. boxes in Fig. 4d and Fig. S2) all contribute to the jet exit strengthening over Europe (Fig. 6a-c). In the region with the strongest zonal wind increase (boxes in Fig. 6), the area-mean tropical cloud impact ($1\,\mathrm{m\,s^{-1}}$) is dominated by EP cloud changes ($0.45\,\mathrm{m\,s^{-1}}$) followed by WP ($0.36\,\mathrm{m\,s^{-1}}$) and IO ($0.23\,\mathrm{m\,s^{-1}}$) cloud changes. In contrast, the impact of tropical Atlantic (TA) cloud changes ($0.07\,\mathrm{m\,s^{-1}}$) is small (Fig. 6d). Over the North Atlantic, EP and TA cloud changes are most important for the pattern of the u_{850} response and the jet strengthening, but all four tropical regions contribute to the poleward jet shift of the North Atlantic jet stream. Note that while dividing the global cloud impact into tropical, midlatitude and polar cloud changes results in a substantial overestimation of the global cloud impact, dividing the tropical cloud impact into WP, EP, IO and TA cloud changes results in a comparably weak overestimation of the tropical cloud impact across the North Atlantic-European region (Fig. 6e-f). The overestimation in the region of the jet exit strengthening amounts to only about 12.5%.

Our results show that no smaller tropical region dominates the tropical cloud-radiative impact on the jet exit strengthening. This result is independent of whether we investigate the sum of the individual cloud impacts or the cloud impact that results from simultaneous cloud changes in the different tropical regions (not shown), and indicates that large-scale processes and interactions, such as the Walker circulation, are important for the circulation response over Europe. Further, the change in atmospheric cloud-radiative heating has a rather complex spatial structure, making it difficult to select smaller regions without introducing heating gradients that might affect the circulation response to tropical cloud-radiative heating.

4 Conclusions

We investigated the atmospheric pathway of the cloud-radiative impact on the zonal wind and jet stream responses to climate change over the North Atlantic-European region during boreal winter. The jet exit strengthening, i.e., the eastward extension of the North Atlantic jet stream towards Europe and the associated zonal wind increase over Europe, is robust across coupled and atmosphere-only climate models and climate change scenarios. At the same time, the zonal wind response over the North Atlantic is not robust. Global cloud-radiative changes contribute robustly to the jet exit strengthening in simulations with the atmospheric components of ICON, MPI-ESM and IPSL-CM5A that apply the cloud- or cloud- and water vapor-locking methods. Further, cloud-radiative heating can be considered as one source of model uncertainty in the zonal wind and jet stream responses over the North Atlantic. Differences in the absolute and relative contributions of the cloud impacts are related to differences in the magnitude and pattern in the upper-tropospheric change in atmospheric cloud-radiative heating in the three models.

Tropical clouds dominate the cloud-radiative impact on the jet exit strengthening in ICON. Indian Ocean, western tropical Pacific and eastern tropical Pacific cloud changes all contribute to the jet exit strengthening while tropical Atlantic cloud changes have a minor impact. This is consistent with the changes in atmospheric cloud-radiative heating, which are largest over the tropical Pacific and Indian Ocean.

Previous studies related the jet shift in response to tropical heating to the development of Rossby wave trains (e.g., Ciasto et al., 2016; Palmer and Mansfield, 1984). Indications of Rossby waves originating from the tropics are seen in particular for the WP and EP cloud-radiative changes, and for these are consistent with the jet responses over the North Atlantic ocean (cf. Figs. S4 and S5 for maps of stationary eddy stream function and meridional wind responses). However, even though all tropical regions show the zonal wind increase over Europe, they exhibit different responses of the stationary eddy stream function over Europe (Fig. S4). Thus, we find no obvious link between the robust cloud-induced jet exit strengthening and Rossby wave trains originating from the tropics.

Our results highlight the importance of cloud-radiative changes, especially those in the tropical upper troposphere, for the midlatitude circulation response to climate change. While cloud-radiative changes support the robust circulation response in some regions, they also contribute to uncertainties in the circulation response in other regions. Future studies should investigate the cloud-radiative impact in coupled climate models, and decompose the cloud-radiative impact into the atmospheric and surface pathways.

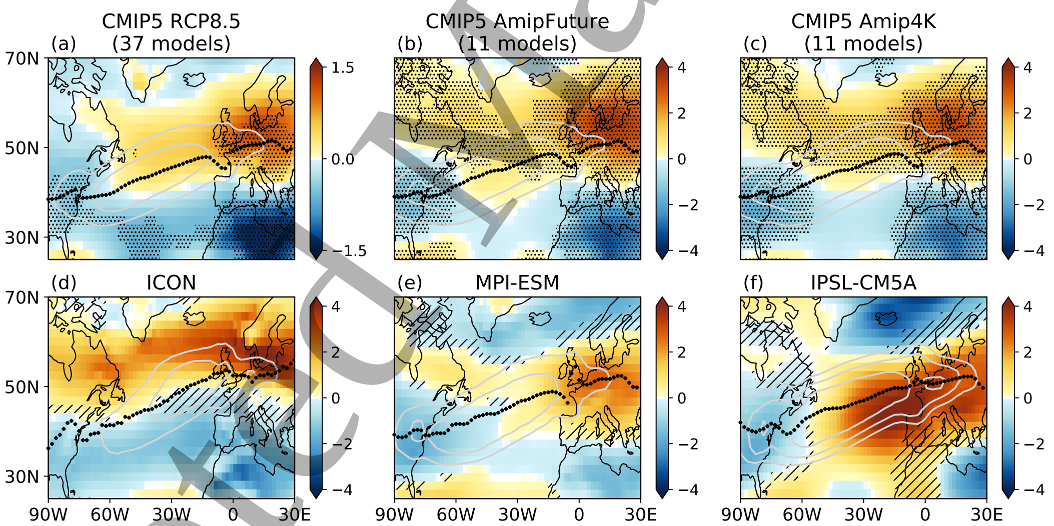

Figure 1: Response of the zonal wind at 850 hPa, u_{850}, to climate change. Shown are the model-mean responses for the RCP8.5 (a), AmipFuture (b) and Amip4K (c) scenarios. The bottom row shows the total locked response to the uniform 4 K SST increase in ICON (d), MPI-ESM (e), and IPSL-CM5A (f). The black dots show the model-mean jet latitude in the historical (a) and Amip (b, c) simulations, as well as in the control simulations of ICON (d), MPI-ESM (e) and IPSL-CM5A (f). The grey contours show the 8, 10 and 12 $\mathrm{m\,s^{-1}}$ u_{850} isolines from the control simulations. Stippling in the first row indicates where more than 80% of the models agree on the sign of the response. Hatching in the bottom panels indicates where the sign of the responses in ICON, MPI-ESM and IPSL-CM5A does not agree with the sign of the robust Amip4K response. Reprinted with permission from Albern (2021).

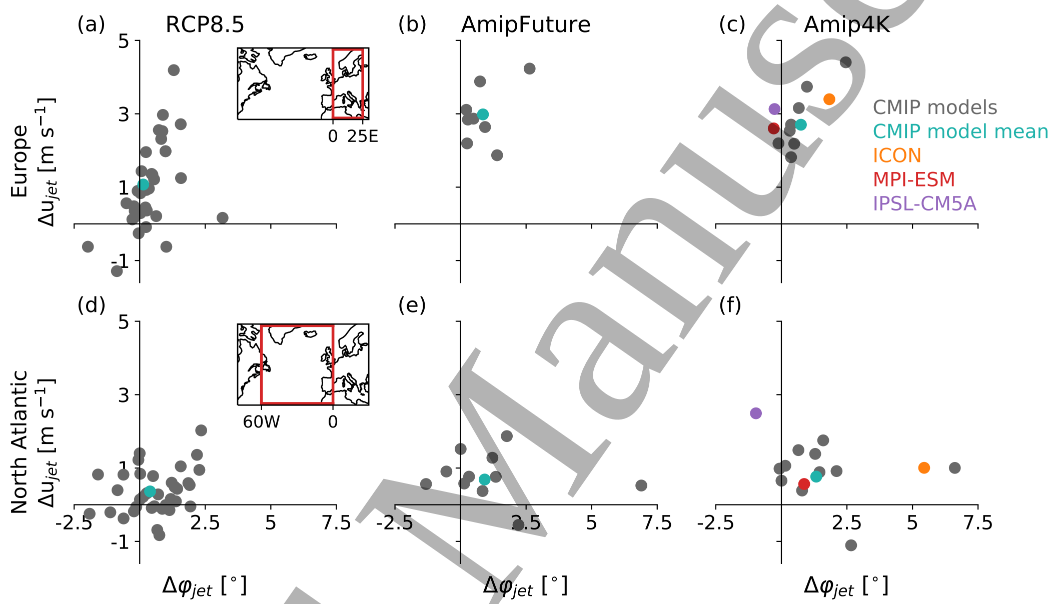

Figure 2: Zonal-mean jet shift $\Delta\varphi_{jet}$ versus jet strengthening Δu_{jet} over Europe (a-c) and over the North Atlantic (d-f). The regions are highlighted in the inserted maps. Depicted are the responses in the individual CMIP5 models and the CMIP5 model mean for the RCP8.5 (a, d), AmipFuture (b, e) and Amip4K (c, f) scenarios. The Amip4K panels also show the total locked responses in ICON, MPI-ESM and IPSL-CM5A. Adapted with permission from Albern (2021).

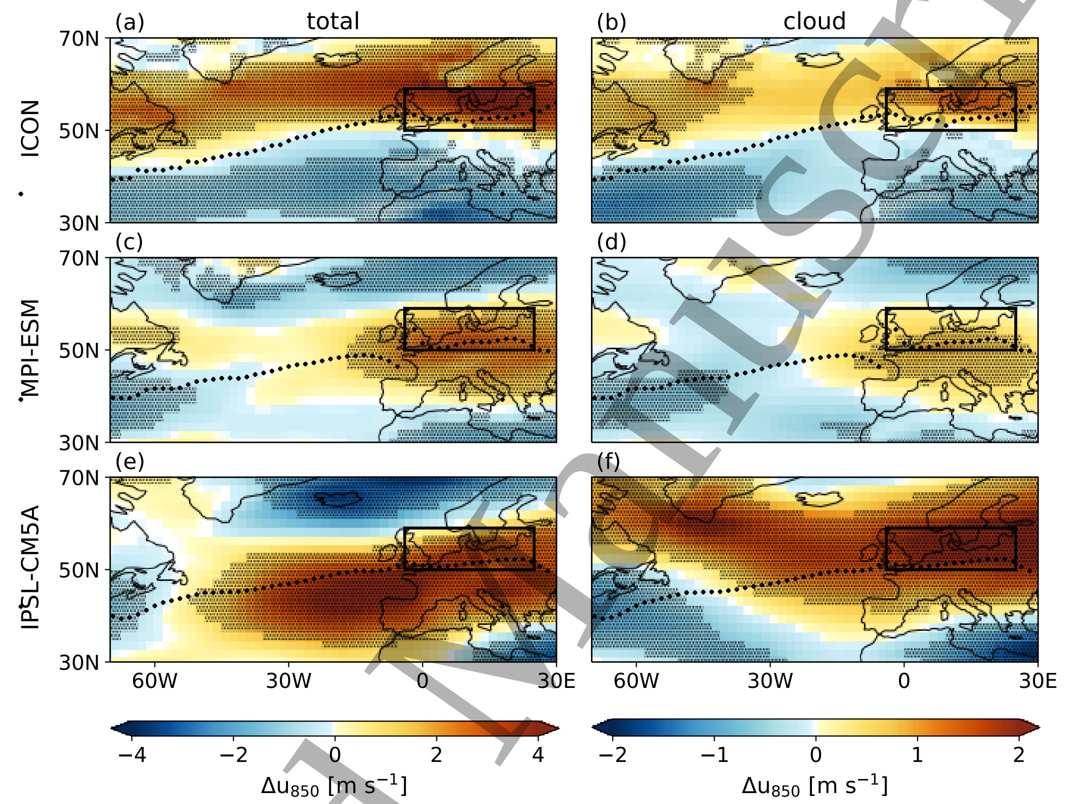

Figure 3: Response of the zonal wind at 850 hPa, Δu_{850}, in ICON (a, b), MPI-ESM (c, d), and IPSL-CM5A (e, f) to a uniform 4 K SST increase. Shown are the total response (a, c, e) and the cloud-radiative impact (b, d, f). Note the different colorbar limits for the two columns. Stippling indicates statistical significance which is determined based on bootstrap calculations as in Albern et al. (2020). The response is statistically significant if the 5th-95th-percentile range of the bootstrap distribution for each grid point does not include $\Delta u_{850} = 0\,\mathrm{m\,s^{-1}}$. The thick black dots indicate the jet latitude in the control simulation with locked clouds. The box indicates the region 50°N-59°N and 4°W-25°E. Adapted with permission from Albern (2021).

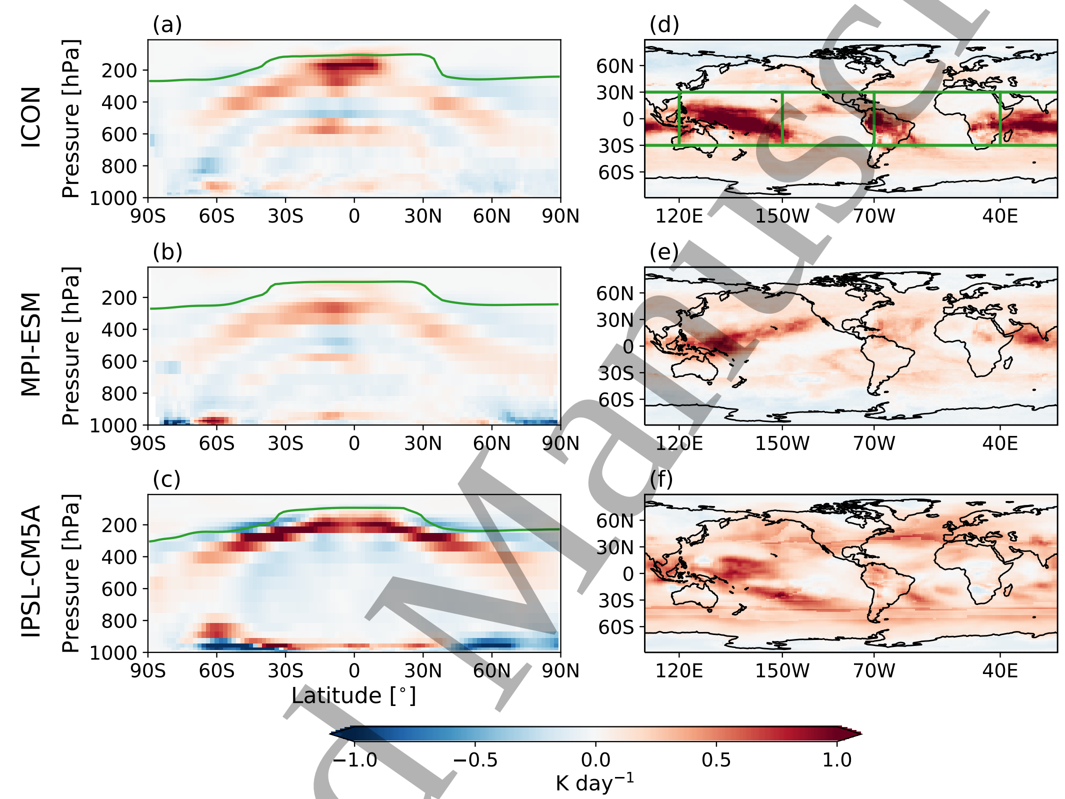

Figure 4: Changes in atmospheric cloud-radiative heating in ICON (a, d), MPI-ESM (b, e), and IPSL-CM5A (c, f). (a-c) Zonal-mean changes. The green lines show the tropopause height in the control simulation. (d-f) Upper-tropospheric vertical-mean changes for a 200-hPa-thick layer below the tropopause. The green boxes in (d) show the tropical regions which are investigated in section 3.2. Adapted with permission from Albern (2021).

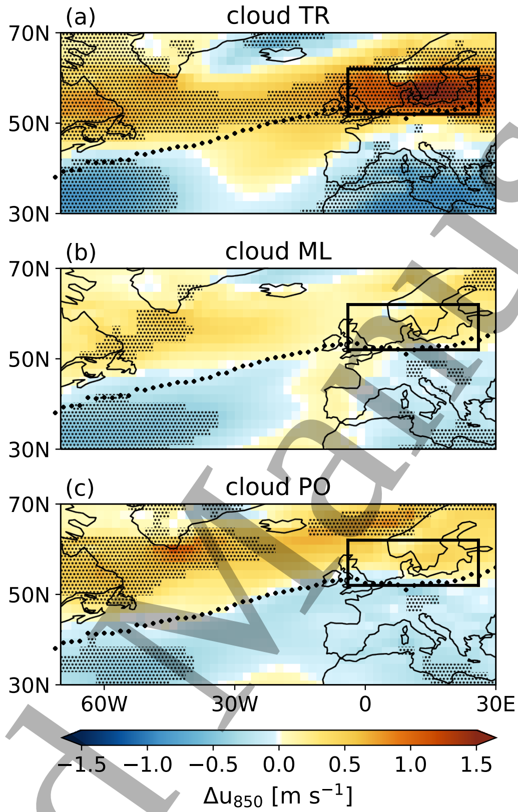

Figure 5: Impact of regional cloud-radiative changes over the (a) tropics, (b) mid-latitudes, and (c) polar regions on the zonal wind response at 850 hPa, Δu_{850}, in the ICON model (cf. Fig. S2 for the regions). Stippling indicates where the response is statistically significant based on the 5th-95th-percentile range of the bootstrap distribution for each grid point. The thick black dots indicate the jet latitude in the control simulation with locked clouds. The box indicates the region 52°N-62°N, 4°W-26°E. Adapted with permission from Albern (2021).

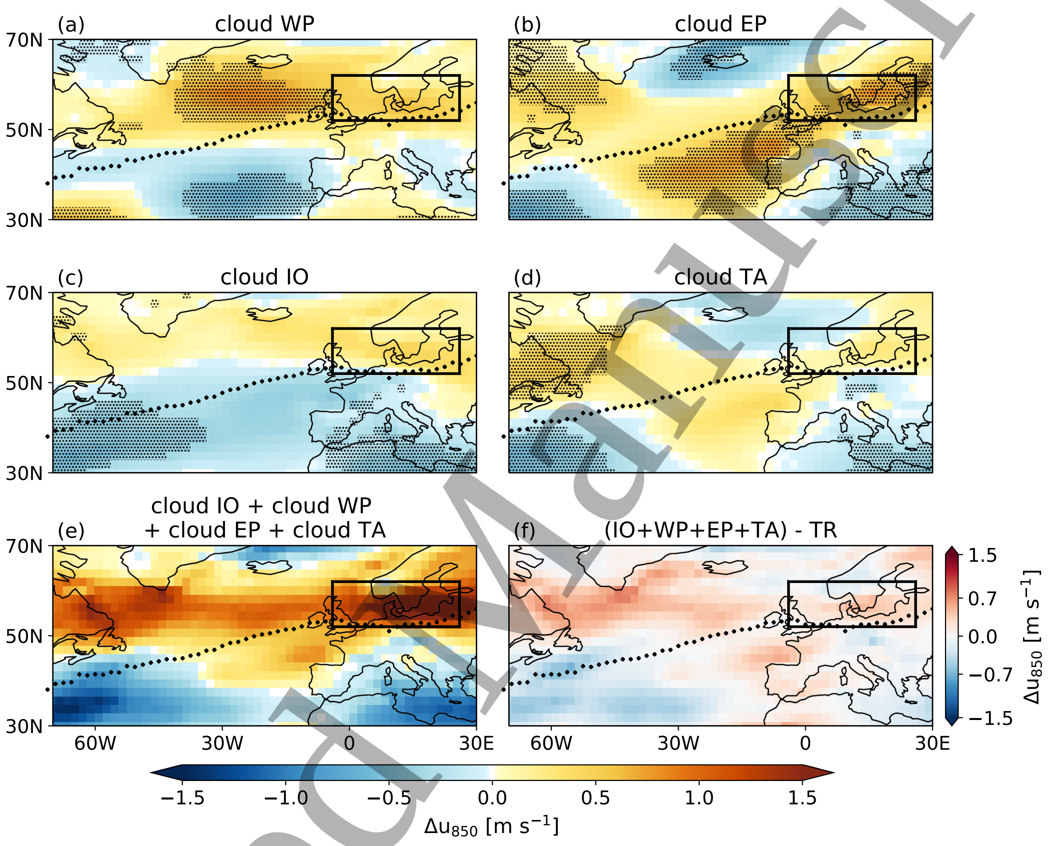

Figure 6: Same as Fig. 5, but for cloud changes over the (a) western tropical Pacific (cloud WP), (b) eastern tropical Pacific (cloud EP), (c) Indian Ocean (cloud IO), and (d) tropical Atlantic (cloud TA). Shown are also (e) the sum of IO, WP, EP, and TA cloud changes and (f) the difference between (e) and the tropical cloud impact shown in Fig. 5a. Adapted with permission from Albern (2021).

Acknowledgments

This article reuses material from N.A.'s dissertation "The radiative impact of clouds on the response of the midlatitude circulation to global warming", published at KITopen from Karlsruhe Institute of Technology with doi 10.5445/IR/1000129873. See Albern (2021) for the full reference.

N.A. and A.V. are supported by the German Ministry of Education and Research (BMBF) and FONA: Research for Sustainable Development (www.fona.de) under grant agreement 01LK1509A. J.G.P. thanks AXA research fund for support. The ICON simulations were carried out by N.A. at the Mistral supercomputer of the German Climate Computing Center (DKRZ) in Hamburg, Germany. The MPI-ESM simulations were carried out by A.V. at the RCC of the University of Chicago. The IPSL-CM5A simulations were performed by A.V. at a Linux cluster of the Lamont-Doherty Earth Observatory. We acknowledge the World Climate Research Programme's Working Group on Coupled Modelling, which is responsible for CMIP, and we thank the climate modeling groups for producing and making available their model output. For CMIP the U.S. Department of Energy's Program for Climate Model Diagnosis and Intercomparison provides coordinating support and led development of software infrastructure in partnership with the Global Organization for Earth System Science Portals. We also thank the developers and maintainers of the open source python libraries numpy, matplotlib, cartopy, netCDF4, Basemap, scipy and pandas which were used for the analysis. This work contributes to the BMBF-funded project "HD(CP)^2: High Definition Clouds and Precipitation for Advancing Climate Prediction".

The analysis scripts and run scripts for the ICON simulations are provided in the Gitlab repository https://gitlab.phaidra.org/albernn21/Albern-etal-clouds-jet-ERL2021 hosted by University of Vienna. Monthly-mean output from the ICON, MPI-ESM and IPSL-CM5A simulations that apply the cloud-locking and cloud- and water vapor-locking methods is published at KITopen with doi 10.5445/IR/1000134626. The KITopen data set also includes a copy of the analysis scripts and run scripts with git commit 9d03f05f7be7f785220c8f662fa64f3dd71a52ec.

References

Albern, N., Voigt, A., and Pinto, J. G. (2019). Cloud-Radiative Impact on the Regional Responses of the Midlatitude Jet Streams and Storm Tracks to Global Warming. *J. Adv. Model. Earth Syst.*, 11(7):1940–1958.

Albern, N., Voigt, A., Thompson, D. W. J., and Pinto, J. G. (2020). The Role of Tropical, Midlatitude, and Polar Cloud-Radiative Changes for the Midlatitude Circulation Response to Global Warming. *J. Climate*, 33(18):7927–7943.

Albern, N. B. S. (2021). *The radiative impact of clouds on the response of the* *midlatitude circulation to global warming.* PhD thesis, Karlsruher Institut für Technologie. DOI: 10.5445/IR/1000129873.

Barnes, E. A. and Polvani, L. M. (2013). Response of the midlatitude jets and of their variability to increased greenhouse gases in CMIP5 models. *J. Climate*, 26:7117–7135.

Butler, A. H., Thompson, D. W., and Heikes, R. (2010). The Steady-State Atmospheric Circulation Response to Climate Change-like Thermal Forcings in a Simple General Circulation Model. *J. Climate*, 23:3474–3496.

Carvalho, D., Rocha, A., Gómez-Gesteira, M., and Silva Santos, C. (2017). Potential impacts of climate change on European wind energy resource under the CMIP5 future climate projections. *Renew. Energy*, 101:29–40.

Catto, J. L., Ackerley, D., Booth, J. F., Champion, A. J., Colle, B. A., Pfahl, S., Pinto, J. G., Quinting, J. F., and Seiler, C. (2019). The Future of Midlatitude Cyclones. *Curr. Clim. Change Rep.*, 5:407–420.

Chang, E. K. M., Guo, Y., and Xia, X. (2012). CMIP5 multimodel ensemble projection of storm track change under global warming. *J. Geophys. Res.*, 117(D23118).

Ciasto, L. M., Li, C., Wettstein, J. J., and Kvamstø, N. G. (2016). North Atlantic Storm-Track Sensitivity to Projected Sea Surface Temperature: Local versus Remote Influences. *J. Climate*, 29(19):6973–6991.

Colman, R. A. and McAvaney, B. J. (1997). A study of general circulation model climate feedbacks determined from perturbed sea surface temperature experiments. *J. Geophys. Res.*, 102(D16):19383–19402.

Dufresne, J.-L., Foujols, M.-A., Denvil, S., Caubel, A., Marti, O., Aumont, O., Balkanski, Y., Bekki, S., Bellenger, H., Benshila, R., Bony, S., Bopp, L., Braconnot, P., Brockmann, P., Cadule, P., Cheruy, F., Codron, F., Cozic, A., Cugnet, D., de Noblet, N., Duvel, J.-P., Ethé, C., Fairhead, L., Fichefet, T., Flavoni, S., Friedlingstein, P., Grandpeix, J.-Y., Guez, L., Guilyardi, E., Hauglustaine, D., Hourdin, F., Idelkadi, A., Ghattas, J., Joussaume, S., Kageyama, M., Krinner, G., Labetoulle, S., Lahellec, A., Lefebvre, M.-P., Lefevre, F., Levy, C., Li, Z. X., Lloyd, J., Lott, F., Madec, G., Mancip, M., Marchand, M., Masson, S., Meurdesoif, Y., Mignot, J., Musat, I., Parouty, S., Polcher, J., Rio, C., Schulz, M., Swingedouw, D., Szopa, S., Talandier, C., Terray, P., Viovy, N., and Vuichard, N. (2013). Climate change projections using the IPSL-CM5 Earth System Model: from CMIP3 to CMIP5. *Clim. Dyn.*, 40:2123–2165.

Eyring, V., Bony, S., Meehl, G. A., Senior, C. A., Stevens, B., Stouffer, R. J., and Taylor, K. E. (2016). Overview of the Coupled Model Intercomparison Project Phase 6 (CMIP6) experimental design and organization. *Geosci. Model Dev.*, 9(5):1937–1958.

Giorgetta, M. A., Jungclaus, J., Reick, C. H., Legutke, S., Bader, J., Böttinger, M., Brovkin, V., Crueger, T., Esch, M., Fieg, K., Glushak, K., Gayler, V., Haak, H., Hollweg, H.-D., Ilyina, T., Kinne, S., Kornblueh, L., Matei, D., Mauritsen, T., Mikolajewicz, U., Mueller, W., Notz, D., Pithan, F., Raddatz, T., Rast, S., Redler, R., Roeckner, E., Schmidt, H., Schnur, R., Segschneider, J., Six, K. D., Stockhause, M., Timmreck, C., Wegner, J., Widmann, H., Wieners, K.-H., Claussen, M., Marotzke, J., and Stevens, B. (2013). Climate and carbon cycle changes from 1850 to 2100 in MPI-ESM simulations for the Coupled Model Intercomparison Project phase 5. *J. Adv. Model. Earth Syst.*, 5(3):572–597.

Harvey, B. J., Cook, P., Shaffrey, L. C., and Schiemann, R. (2020). The response of the northern hemisphere storm tracks and jet streams to climate change in the CMIP3, CMIP5, and CMIP6 climate models. *J. Geophys. Res. Atmos.*, 125(23):e2020JD032701.

Harvey, B. J., Shaffrey, L. C., and Woollings, T. J. (2015). Deconstructing the climate change response of the Northern Hemisphere wintertime storm tracks. *Clim. Dyn.*, 45(9):2847–2860.

Hueging, H., Haas, R., Born, K., Jacob, D., and Pinto, J. G. (2013). Regional Changes in Wind Energy Potential over Europe Using Regional Climate Model Ensemble Projections. *J. Appl. Meteorol. Climatol.*, 52(4):903–917.

Leckebusch, G. C., Ulbrich, U., Fröhlich, L., and Pinto, J. G. (2007). Property loss potentials for European midlatitude storms in a changing climate. *Geophys. Res. Lett.*, 34(5).

Lee, S. H., Williams, P. D., and Frame, T. H. A. (2019). Increased shear in the North Atlantic upper-level jet stream over the past four decades. *Nature*, 572:639–642.

Meehl, G. A., Boer, G. J., Covey, C., Latif, M., and Stouffer, R. J. (2000). The Coupled Model Intercomparison Project (CMIP). *Bull. Amer. Meteor. Soc.*, 81(2):313–318.

Moemken, J., Reyers, M., Feldmann, H., and Pinto, J. G. (2018). Future Changes of Wind Speed and Wind Energy Potentials in EURO-CORDEX Ensemble Simulations. *J. Geophys. Res. Atmos.*, 123(12):6373–6389.

Palmer, T. N. and Mansfield, D. A. (1984). Response of two atmospheric general circulation models to sea-surface temperature anomalies in the tropical East and West Pacific. *Nature*, 310:483–485.

Pinto, J. G., Karremann, M. K., Born, K., Della-Marta, P. M., and Klawa, M. (2012). Loss potentials associated with European windstorms under future climate conditions. *Clim. Res.*, 54:1–20.

Pinto, J. G., Ulbrich, U., Leckebusch, G. C., Spangehl, T., Reyers, M., and Zacharias, S. (2007). Changes in storm track and cyclone activity in three SRES ensemble experiments with the ECHAM5/MPI-OM1 GCM. *Clim. Dyn.*, 29(2):195–210.

Reyers, M., Moemken, J., and Pinto, J. G. (2016). Future changes of wind energy potentials over Europe in a large CMIP5 multi-model ensemble. *Int. J. Climatol.*, 36(2):783–796.

Shepherd, T. G. (2014). Atmospheric circulation as a source of uncertainty in climate change projections. *Nature Geosci.*, 7:703–708.

Simpson, I. R., Shaw, T. A., and Seager, R. (2014). A Diagnosis of the Seasonally and Longitudinally Varying Midlatitude Circulation Response to Global Warming. *J. Atmos. Sci.*, 71:2489–2515.

Stevens, B., Giorgetta, M., Esch, M., Mauritsen, T., Crueger, T., Rast, S., and Roeckner, E. (2013). Atmospheric component of the MPI-M Earth System Model: ECHAM6. *J. Adv. Model. Earth Syst.*, 5:146–172.

Taylor, K. E., Stouffer, R. J., and Meehl, G. A. (2009). A Summary of the CMIP5 Experiment Design. *PCMDI Reports*.

Taylor, K. E., Stouffer, R. J., and Meehl, G. A. (2012). An Overview of CMIP5 and the Experiment Design. *Bull. Amer. Meteor. Soc.*, 93:485–498.

Vallis, G. K., Zurita-Gotor, P., Cairns, C., and Kidston, J. (2015). Response of the large-scale structure of the atmosphere to global warming. *Q. J. R. Meteorol. Soc.*, 141:1479–1501.

Voigt, A. and Albern, N. (2019). No Cookie for Climate Change. *Geophys. Res. Lett.*, 46(24):14751–14761.

Voigt, A., Albern, N., Ceppi, P., Grise, K., Li, Y., and Medeiros, B. (2021). Clouds, radiation and atmospheric circulation in the present-day climate and under climate change. *WIREs Clim. Change*, 12(2):e694.

Voigt, A., Albern, N., and Papavasileiou, G. (2019). The atmospheric pathway of the cloud-radiative impact on the circulation response to global warming: important and uncertain. *J. Climate*, 32(10):3051–3067.

Voigt, A. and Shaw, T. A. (2015). Circulation response to warming shaped by radiative changes of clouds and water vapor. *Nature Geosci.*, 8:102–106.

Voigt, A. and Shaw, T. A. (2016). Impact of regional atmospheric cloud-radiative changes on shifts of the extratropical jet stream in response to global warming. *J. Climate*, 29(23):8399–8421.

Wetherald, R. T. and Manabe, S. (1988). Cloud Feedback Processes in a General Circulation Model. *J. Atmos. Sci.*, 45(8):1397–1416.

Woollings, T. and Blackburn, M. (2012). The North Atlantic Jet Stream under Climate Change and Its Relation to the NAO and EA Patterns. *J. Climate*, 25(3):886–902.

Zängl, G., Reinert, D., Ripodas, P., and Baldauf, M. (2015). The ICON (ICOsahedral Non-hydrostatic) modelling framework of DWD and MPI-M: Description of the non-hydrostatic dynamical core. *Q. J. R. Meteorol. Soc.*, 141:563–579.

Zappa, G., Hoskins, B. J., and Shepherd, T. G. (2015). Improving Climate Change Detection through Optimal Seasonal Averaging: The Case of the North Atlantic Jet and European Precipitation. *J. Climate*, 28(16):6381–6397.

Zappa, G., Shaffrey, L. C., Hodges, K. I., Sansom, P. G., and Stephenson, D. B. (2013). A Multimodel Assessment of Future Projections of North Atlantic and European Extratropical Cyclones in the CMIP5 Climate Models. *J. Climate*, 26(16):5846–5862.